BLIND BEAMFORMING TECHNIQUES FOR AUTOMATIC IDENTIFICATION SYSTEM USING GSVD AND TRACKING

Mu Zhou and Alle-Jan van der Veen

Delft University of Technology, Dept. of Elec. Eng., Mekelweg 4, 2628 CD Delft, The Netherlands.
Email: zhoumu1301@gmail.com; a.j.vanderveen@tudelft.nl

The automatic identification system (AIS) is a wireless synchronous narrowband communication system for exchanging navigational data through short messages between ships and base stations in the maritime VHF frequency band. The service coverage of each communication cell is limited within the horizon by the line of sight propagation of VHF signals. AIS receivers are put on high buildings besides harbors, lighthouses along coastlines and even on LEO satellites in space to detect signals from more cells. The toughest problem that these receivers are facing is the partial overlapping of messages from multiple cells. Antenna arrays are used in AIS receivers to suppress the interference. A good beamforming algorithm is needed for computing beamformers. Previously, we proposed blind beamforming techniques based on subspace intersection to solve this problem. In this paper, we propose more simple and efficient blind beamforming techniques using the generalized singular value decomposition (GSVD) and its tracking version for the same problem. The proposed algorithms are simulated in an exact dynamic AIS software model, and are tested on real-world AIS signals collected from our experimental hardware. Simulation results show that the proposed algorithms achieve satisfactory performance. Experimental results confirm the effectiveness of the proposed algorithms.

Index Terms— Blind beamforming, automatic identification system, generalized singular value decomposition, signed URV algorithm, subspace tracking

1 INTRODUCTION

The automatic identification system (AIS) is a wireless synchronous narrowband communication system for exchanging navigational data through short messages between ships and base stations. The system is divided into multiple ground cells. Each cell can have a base station. In each cell, the transmission is synchronized by the base station through the self-organized time division multiple access (SOTDMA) technique. The service coverage of each cell is limited within the horizon seen by the base station by the line of sight propagation of the VHF signals. The system covers the area including inland rivers, lakes and the water about 20 to 30 nautical miles off the coastline. The vast area of the open sea is not covered so the ships at sea cannot be detected for no base station is available there.

To detect signals as far as possible, AIS receivers are put on high buildings besides harbors, on lighthouses along coastlines and even on LEO satellites in space. Possibly, one such receiver covers more than one cell. The received messages are getting more and more asynchronous when more cells are covered. The power and delays of the received signals vary in a large range (can be up to 40 dB on high buildings). Even worse, on the LEO satellites, the large variance in Doppler frequency shifts are produced on the received signals [1, 2, 3, 4]. A key problem is the collision of messages from multiple cells. From multiple cells, the messages transmitted from the same time slot are nearly fully overlapping (called Type 1 collision), while the messages from the adjacent time slots can be partially overlapping (called Type 2 collision). Although in the protocol ([5]) Type 2 collision is not supposed to happen if the transmission is within the range of 200 nautical miles, the partial overlapping case is still witnessed in the real-world AIS signals from the harbor of Rotterdam, one of the busiest harbors in the world. This may be due to the poor synchronization devices in transceivers and the small irregular service coverage of actual cells in a complex urban environment. Type 2 collision is the toughest problem for us.

Many papers [6, 7, 8, 9] discussed the use of a simple receiver equipped with only one antenna to detect AIS signals in such harsh environment. It is known that this type of receivers is designed for communication in one cell. Receivers with antenna arrays are candidates for separating the overlapping messages. Algorithms relaying on known training sequences [10, 11, 12, 13] is not efficient for solving the problem since the communication is asynchronous and the training sequence is not unique for each message. The papers [1, 14] make use of classic DOA estimation and beamforming techniques on linear arrays to separate the messages. These techniques require precise calibration and a known beam pattern of the array. In the case of a LEO satellite, additional calibration is nearly impossible once the satellite is launched. Moreover, these techniques cannot distinguish between complete messages and incomplete messages and thus waste processing complexity on the incomplete messages.

In [15], we proposed blind beamforming techniques to suppress the interference. This paper proposes more simple and efficient blind beamforming techniques using the generalized singular value decomposition (GSVD) and its tracking version to further improve the performance.

2 DATA MODEL

In AIS, a frame equal to one minute is divided into 2250 time slots. One message can occupy up to five consecutive time slots but most of the messages are default messages occupying one time slot. A default message is $N_p = 256$ bits long, and this is also the length of a time slot. The default messages are of the most interest for us for the embedded information related to the ships' movement and positions. The binary sequence $\{b[n]\}_{1\leq n\leq N_p}$ of a message is mapped to $\{+1, -1\}$ and then differentially encoded as $a[n] = b[n]a[n-1]$, $n \geq 1$, $a[0] = +1$. The encoded message is Gaussian minimum shift keying (GMSK) [16] modulated and transmitted at rate 9.6 kbps on carriers at frequency 162 MHz. The baseband representation of the transmitted AIS signals has a constant envelope form as

$$\tilde{s}(t) = e^{j\theta(t)}, \tag{1}$$

This work was supported in part by China Scholarship Council from P.R.China.

978-1-4799-2893-4/14/$31.00 ©2014 IEEE

where $\theta(t)$ is the phase given by

$$\theta(t) = \pi h \int_{-\infty}^{t} \sum_{n=-\infty}^{+\infty} a[n] g(\tau - nT) d\tau, \tag{2}$$

where h is the modulation index equal to 0.5, and $g(t)$, a pulse of unit area, is the response of a Gaussian filter to a unit amplitude rectangular pulse of duration T, where T is the symbol period.

Assume an antenna array with M elements. There are d signals, and they are stacked in a vector $\mathbf{s}[k] = [s_1[k], \cdots, s_d[k]]^T$. The received signal vector is

$$\mathbf{x}[k] = \mathbf{h}_1 s_1[k] + \cdots + \mathbf{h}_d s_d[k] + \mathbf{n}[k] = \mathbf{H}\mathbf{s}[k] + \mathbf{n}[k], \tag{3}$$

where the vectors $\mathbf{h}_i$ are the channel vectors (array response vectors) corresponding to each signal, $\mathbf{H} = [\mathbf{h}_1, \cdots, \mathbf{h}_d] \in \mathbb{C}^{M \times d}$ is the channel matrix, and $\mathbf{n} \in \mathbb{C}^M$ is the noise vector. The channel vectors are all scaled to $\|\mathbf{h}_i\| = 1$. The signal power are absorbed into the sources. The noise is assumed to be i.i.d. zero mean Gaussian vectors, with covariance matrix $\mathbf{R}_n = \mathrm{E}(\mathbf{n}\mathbf{n}^H) = \sigma^2\mathbf{I}$. The noise power σ^2 is assumed known. The extent of message overlapping is described as the overlapping ratio (OVR)

$$r_i = \frac{L_i}{N_p} \tag{4}$$

where L_i is the number of overlapping samples of two messages. On our building, the OVR of Type 2 collision is seen typically less than 50%. For a LEO satellite orbiting at altitude 600 km, theoretically, the OVR of Type 2 collision can be up to 29%. In fact, the OVR can be arbitrary but typically less than 50%.

Periodically, a block of data corresponding to an analysis window are collected and processed. Due to the lack of synchronization, the length of the analysis window is set longer than one time slot to collect enough samples of the interference messages from adjacent time slots (See Fig. 1). If we have collected N_s samples $\mathbf{x}[k]$ for the analysis window, then we can push these into a matrix $\mathbf{X} = [\mathbf{x}[1], \cdots, \mathbf{x}[N_s]]$, and similarly for the signals and the noise. The data model corresponding to (3) is

$$\mathbf{X} = \mathbf{H}\mathbf{S} + \mathbf{N} \tag{5}$$

The length of the analysis window is typically set to $N_s = 2N_p$ if sampled at period T. The group of complete messages around the center of the analysis window are the target messages for this analysis window. The target messages are likely transmitted from the same time slot. Other messages are incomplete and are treated as interference for this analysis window. The interference messages are mainly transmitted from adjacent time slots. The interference messages in the current analysis window can be target messages in adjacent analysis windows if the spacing between analysis windows is about $0.5N_p$. When the coordinated universal time (UTC) is available (such as GPS 1 pps signal), the positions of the analysis windows can be aligned with UTC.

3 Blind Beamforming Techniques

The interference messages make the data of the analysis window nonstationary and cause difficulty for classic algorithms. The principle of our algorithms is to divide the analysis window into two sub-blocks. The messages as well as the related subspaces are classified into two groups, target messages and interference messages, by comparing the power of the messages in the two sub-blocks. To identify the messages, we define the distinction between the target

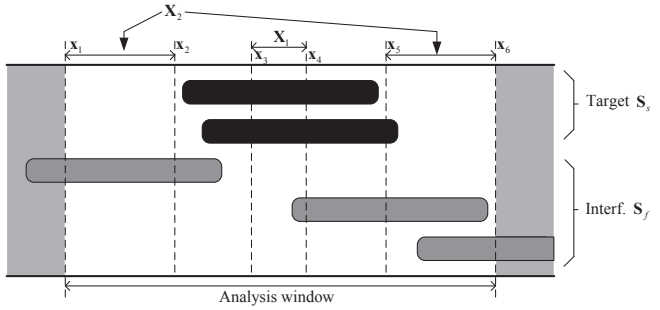

Fig. 1. The scenario and the analysis window.

messages and the interference messages as follows. From the analysis window, we form two matrices $\mathbf{X}_1$: $M \times N_1$ and $\mathbf{X}_2$: $M \times N_2$ as (See Fig. 1)

$$\begin{array}{rcl} \mathbf{X}_1 & = & \mathbf{H}_s\mathbf{S}_{s1} + \mathbf{H}_f\mathbf{S}_{f1} + \mathbf{N}_1 = \mathbf{H}\mathbf{S}_1 + \mathbf{N}_1 \\ \mathbf{X}_2 & = & \mathbf{H}_s\mathbf{S}_{s2} + \mathbf{H}_f\mathbf{S}_{f2} + \mathbf{N}_2 = \mathbf{H}\mathbf{S}_2 + \mathbf{N}_2 \end{array} \tag{6}$$

where $\mathbf{H} = [\mathbf{H}_s\, \mathbf{H}_f]$ and $\mathbf{S}_i = [\mathbf{S}_{si}^T\, \mathbf{S}_{fi}^T]^T$, $i = 1, 2$. $\mathbf{H}_s$ and $\mathbf{H}_f$ are the channel matrices of the target messages and the interference messages, respectively. $\mathbf{S}_{si}$: $d_s \times N_i$ and $\mathbf{S}_{fi}$: $d_f \times N_i$ are the source data matrices containing the target messages and the interference messages, respectively. Two corresponding sample covariance matrices are formed as (the cross-correlation items are ignored)

$$\begin{array}{rcl} \hat{\mathbf{R}}_1 & = & \frac{1}{N_1}\mathbf{X}_1\mathbf{X}_2^H \\ & \approx & \frac{1}{N_1}(\mathbf{H}_s\mathbf{S}_{s1}\mathbf{S}_{s1}^H\mathbf{H}_s^H + \mathbf{H}_f\mathbf{S}_{f1}\mathbf{S}_{f1}^H\mathbf{H}_f^H + \mathbf{N}_1\mathbf{N}_1^H) \\ \hat{\mathbf{R}}_2 & = & \frac{1}{N_2}\mathbf{X}_2\mathbf{X}_2^H \\ & \approx & \frac{1}{N_2}(\mathbf{H}_s\mathbf{S}_{s2}\mathbf{S}_{s2}^H\mathbf{H}_s^H + \mathbf{H}_f\mathbf{S}_{f2}\mathbf{S}_{f2}^H\mathbf{H}_f^H + \mathbf{N}_2\mathbf{N}_2^H) \end{array} \tag{7}$$

The distinction is defined as

$$\left\{ \begin{array}{rcl} \alpha^2\mathbf{S}_{s1}\mathbf{S}_{s1}^H & > & \mathbf{S}_{s2}\mathbf{S}_{s2}^H \\ \alpha^2\mathbf{S}_{f1}\mathbf{S}_{f1}^H & < & \mathbf{S}_{f2}\mathbf{S}_{f2}^H \end{array} \right. \tag{8}$$

where α is a scaling factor to make the scaled power of the matrices satisfying the inequalities for given $\mathbf{S}_{si}$ and $\mathbf{S}_{fi}$. The power of $\mathbf{S}_{si}$ and $\mathbf{S}_{fi}$ depends on the split parts of the messages. α is determined from a marginal case of this splitting. In a marginal case, a target message should be detected when one part of this message fills up $\mathbf{X}_1$ and the other part fills up $\mathbf{X}_2$ (messages could occupy two time slots). In this case, the length of $\mathbf{S}_{s1}$ is N_1 and the length of $\mathbf{S}_{s2}$ is N_2. The first inequality in (8) is used to compute α. Through some complex deduction, we have the lower bound of α as

$$\alpha > \frac{\sqrt{N_2} + \sqrt{M}}{\sqrt{N_1} - \sqrt{M}} \tag{9}$$

Here, α is normally preferred to be as close to the lower bound as possible. To implement this classification of messages, we take the GSVD of $\mathbf{X}_1$ and $\mathbf{X}_2$ as

$$\mathrm{GSVD}(\mathbf{X}_1, \mathbf{X}_2) \Leftrightarrow \left\{ \begin{array}{rcl} \mathbf{X}_1 & = & \mathbf{F}\mathbf{C}\mathbf{U}^H \\ \mathbf{X}_2 & = & \mathbf{F}\mathbf{S}\mathbf{V}^H \end{array} \right. \tag{10}$$

where $\mathbf{F}$: $M \times M$ is an invertible matrix with the norm of each column scaled to 1, $\mathbf{C}$ and $\mathbf{S}$ are square positive diagonal matrices, and $\mathbf{U}$: $N_1 \times M$ and $\mathbf{V}$: $N_2 \times M$ are semi-unitary matrices. For a

given threshold $\epsilon \geq 0$, we sort the generalized singular values and partition of $\mathbf{F}$, $\mathbf{C}$, $\mathbf{S}$ as

$$\mathbf{F} = [\mathbf{F}_1\, \mathbf{F}_2\, \mathbf{F}_3] \tag{11}$$

$$\mathbf{C} = \begin{bmatrix} \mathbf{C}_1 & & \\ & \mathbf{C}_2 & \\ & & \mathbf{C}_3 \end{bmatrix} \quad \begin{matrix} \mathbf{C}_1 > \epsilon\mathbf{I} \\ \\ \mathbf{C}_3 < \epsilon\mathbf{I} \end{matrix} \tag{12}$$

$$\mathbf{S} = \begin{bmatrix} \mathbf{S}_1 & & \\ & \mathbf{S}_2 & \\ & & \mathbf{S}_3 \end{bmatrix} \quad \begin{matrix} \mathbf{S}_2 > \epsilon\mathbf{I} \\ \mathbf{S}_3 < \epsilon\mathbf{I} \end{matrix} \tag{13}$$

where the partitioning corresponding to (8) is

$$\mathbf{C}_1 > \alpha\mathbf{S}_1, \mathbf{C}_2 < \alpha\mathbf{S}_2 \tag{14}$$

If squaring (10) and comparing it with (7), we have the estimates for $\mathbf{H}_s$ and $\mathbf{H}_f$

$$\mathrm{ran}(\mathbf{F}_1) \approx \mathrm{ran}(\mathbf{H}_s),\ \mathrm{ran}(\mathbf{F}_2) \approx \mathrm{ran}(\mathbf{H}_f) \tag{15}$$

$\mathrm{ran}(*)$ denotes the column range of a matrix. In noiseless cases with N_p long enough, the approximation in (15) is replaced by equalities. The number of the target messages d_s (equal to the rank of $\mathbf{F}_1$) is naturally estimated from the GSVD. From $\mathbf{F}$, we can construct an oblique projector [17, 18] to suppress the interference

$$\mathbf{E} = [\mathbf{F}_1\, \mathbf{F}_2] \begin{bmatrix} \mathbf{I} & \\ & \mathbf{0} \end{bmatrix} [\mathbf{F}_1\, \mathbf{F}_2]^\dagger \tag{16}$$

where "†" denotes the pseudo-inverse. The separating beamformer to suppress the interference is constructed as

$$\mathbf{W}^{(1)H} = [\mathbf{I}\,\mathbf{0}][\mathbf{F}_1\, \mathbf{F}_2]^\dagger = (\mathbf{F}_1^H \mathbf{P}_f^\perp \mathbf{F}_1)^{-1} \mathbf{F}_1^H \mathbf{P}_f^\perp \tag{17}$$

where $\mathbf{P}_f^\perp = \mathbf{I} - \mathbf{F}_2\mathbf{F}_2^\dagger = \mathbf{I} - \mathbf{F}_2(\mathbf{F}_2^H\mathbf{F}_2)^{-1}\mathbf{F}_2^H$. This beamformer maximizes the output power of the target signals. More generally, we can construct another oblique projector to suppress the interference

$$\mathbf{E} = \mathbf{F} \begin{bmatrix} \mathbf{I} & & \\ & \mathbf{0} & \\ & & \mathbf{0} \end{bmatrix} \mathbf{F}^{-1} \tag{18}$$

The corresponding separating beamformer to suppress the interference is constructed as

$$\mathbf{W}^{(1)H} = [\mathbf{I}\,\mathbf{0}\,\mathbf{0}]\mathbf{F}^{-1} \tag{19}$$

The beamformer (17) is a special case of the beamformer (19) when $\mathrm{ran}(\mathbf{F}_3)$ is orthogonal to $\mathrm{ran}([\mathbf{F}_1\, \mathbf{F}_2])$. The beamformer (19) gives us more freedom to design algorithms.

The subspace estimates from the GSVD are special cases of the Schur subspace estimate 2 (SSE-2) [19], which is computed through the signed URV algorithm (SURV) [20]. The proof is not shown here but it is very similar to the proof of the SVD being a special case of SSE-2 [20]. We can alternatively compute the beamformer from the decomposition $\mathrm{SURV}\,(\gamma\overset{j_\gamma}{\mathbf{I}}, \alpha\overset{+}{\mathbf{X}}_1, \overset{-}{\mathbf{X}}_2)$ as

$$\mathbf{Q}^H\, [\gamma\overset{j_\gamma}{\mathbf{I}}\ \alpha\overset{+}{\mathbf{X}}_1\ \ \overset{-}{\mathbf{X}}_2]\, \mathbf{\Theta} = \mathbf{Q}^H\ \overset{+}{[\mathbf{A}}\ \ \overset{+}{\mathbf{0}}\ |\ \overset{-}{\mathbf{B}}\ \ \overset{-}{\mathbf{0}}] = \overset{+}{[\mathbf{R}_\mathbf{A}}\ \ \overset{+}{\mathbf{0}}\ |\ \overset{-}{\mathbf{R}_\mathbf{B}}\ \ \overset{-}{\mathbf{0}}] \tag{20}$$

where the sign "$\pm$" and j_γ above the matrices denote the signatures of the columns of the matrices, $\mathbf{\Theta}$ is a $\mathbf{J}$-unitary matrix, $\mathbf{Q}$ is a unitary matrix, $\mathbf{A}$: $M \times d_s$ and $\mathbf{B}$: $M \times (M - d_s)$, $\mathbf{R}_\mathbf{A}$: $M \times d_s$ and $\mathbf{R}_\mathbf{B}$: $M \times (M - d_s)$ together are lower triangular, and γ is a threshold to balance the scaled noise power in $\alpha\mathbf{X}_1$ and $\mathbf{X}_2$ and to keep the noise subspace in the negative part of the SURV. γ is given as

$$\gamma = \sqrt{|t|},\ \begin{cases} j_\gamma = -1, \text{ when } t > 0; \\ j_\gamma = +1, \text{ when } t \leq 0. \end{cases} \tag{21}$$

$$t = \sigma^2 \left[\alpha^2 \left(\sqrt{N_1} + \sqrt{M}\right)^2 - \left(\sqrt{N_2} - \sqrt{M}\right)^2\right] \tag{22}$$

$\mathrm{ran}(\mathbf{A}) \approx \mathrm{ran}(\mathbf{F}_1)$ and $\mathrm{ran}(\mathbf{B}) \approx \mathrm{ran}([\mathbf{F}_2\, \mathbf{F}_3])$. Let $\mathbf{Q} = [\mathbf{Q}_\mathbf{A}\, \mathbf{Q}_\mathbf{B}]$ be partitioned according to $[\mathbf{R}_\mathbf{A}\, \mathbf{R}_\mathbf{B}]$. The separating beamformer is given as

$$\mathbf{W}^{(1)H} = [\mathbf{I} \quad \mathbf{0}][\mathbf{A} \quad \mathbf{B}]^\dagger = (\mathbf{A}^H \mathbf{P}_\mathbf{B}^\perp \mathbf{A})^{-1} \mathbf{A}^H \mathbf{P}_\mathbf{B}^\perp . \tag{23}$$

where $\mathbf{P}_\mathbf{B}^\perp = \mathbf{I} - \mathbf{B}\mathbf{B}^\dagger$. The factor $(\mathbf{A}^H\mathbf{P}_\mathbf{B}^\perp\mathbf{A})^{-1}$ is invertible and can be omitted without changing the effect of the beamformer, and $\mathbf{A} = \mathbf{Q}\mathbf{R}_\mathbf{A}$ and $\mathbf{P}_\mathbf{B}^\perp = \mathbf{Q}_\mathbf{A}\mathbf{Q}_\mathbf{A}^H$. We find

$$\begin{aligned} \mathbf{W}^{(1)H} \rightarrow \mathbf{A}^H\mathbf{P}_\mathbf{B}^\perp &= \mathbf{R}_\mathbf{A}\mathbf{Q}^H\mathbf{Q}_\mathbf{A}\mathbf{Q}_\mathbf{A}^H = \mathbf{R}_\mathbf{A}^H \begin{bmatrix} \mathbf{I} \\ \mathbf{0} \end{bmatrix} \mathbf{Q}_\mathbf{A}^H \\ &= \mathbf{R}'_\mathbf{A}\mathbf{Q}_\mathbf{A}^H \rightarrow \mathbf{Q}_\mathbf{A}^H \end{aligned} \tag{24}$$

Herein, $\mathbf{R}'_\mathbf{A}$ is a square lower-triangular matrix (the top part of $\mathbf{R}_\mathbf{A}$), and because being invertible, it can be omitted.

The interference messages are suppressed as

$$\mathbf{X}^{(1)} = \mathbf{W}^{(1)H}\mathbf{X} \tag{25}$$

The block stationary data in the middle of $\mathbf{X}^{(1)}$ are passed to algebraic constant modulus algorithm (ACMA) [21] to compute the individual beamformers $\mathbf{W}^{(2)H}$ for the target messages. The overall beamformer is found as

$$\mathbf{W}^H = \mathbf{W}^{(2)H}\mathbf{W}^{(1)H} \tag{26}$$

and the target messages are recovered as

$$\hat{\mathbf{S}}_s = \mathbf{W}^H\mathbf{X} \tag{27}$$

4 GSVD Tracking

Fixed analysis windows aligned to the time slots can be used if UTC is available. An adaptive analysis window is preferable when UTC is not available. The analysis window can be moved column by column ($\mathbf{x}[k]$). The block data are only output and beamformed when a stationary part of the rank estimate is detected. The stationary part is a time period that the estimated number of target messages $\hat{d}_s$ remains unchanged for $0.25N_p$ samples since the last rank changes.

The updating of the window and the decomposition (20) is the same to an ordinary updating of SURV [20, 22]. When the analysis window advancing 1 column, 6 column vectors need to be updated, 1 incoming and 1 leaving vectors for $\mathbf{X}_1$ and 2 incoming and 2 leaving vectors for $\mathbf{X}_2$ (See Fig. 1). We can form this updating of (20) as

$$\mathrm{SURV}\,(\overset{+}{[\mathbf{A}}, \mathbf{x}_1, \alpha\overset{+}{\mathbf{x}_4}, \mathbf{x}_5], \overset{-}{[\mathbf{B}}, \mathbf{x}_2, \alpha\overset{-}{\mathbf{x}_3}, \mathbf{x}_6]) \tag{28}$$

5 Results

In this section, we show the performance of the proposed beamforming algorithms in two scenarios. One is an AIS receiver on a LEO satellite orbiting at altitude 600 km high, and another is an AIS receiver on our building facing the harbor of Rotterdam.

First, we simulate the proposed beamforming algorithms in an exact dynamic AIS software model for a LEO satellite (See [15, 23]). Ships are randomly distributed in the satellite field of view (FoV) and are moving in the opposite direction of the satellite velocity vector. The number of the ships in FoV is kept constant. The antenna

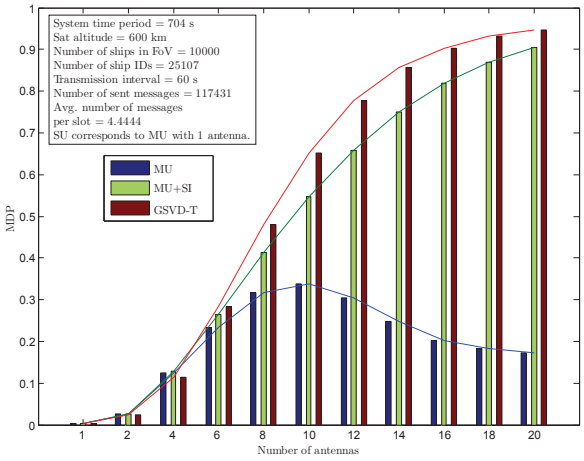

Fig. 2. The performance of the receivers with 10,000 ships in FoV.

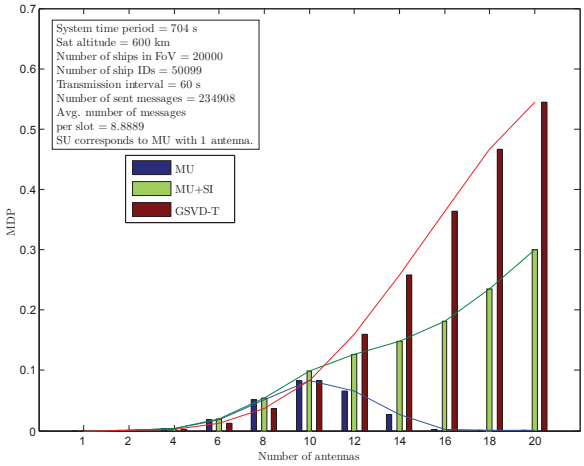

Fig. 3. The performance of the receivers with 20,000 ships in FoV.

array consists of two linear subarrays crossing each other and locating in the plane parallel to FoV. One of the subarrays is parallel to the satellite velocity vector. Each subarray has $M/2$ dipole antennas spacing at half wavelengths. The single user receiver to decode the messages is the same to that in [15]. The time interval between the messages from one ship is 60 seconds. The simulation time is 704 seconds. The performance measure is the message detection probability (MDP), the ratio of the number of successfully decoded messages to the number of sent messages. We set $N_1 = 0.25N_p$ and $N_2 = N_p$ for the proposed GSVD tracking algorithm.

Fig. 2 and Fig. 3 show the performance of the receivers with different beamforming algorithms with 10,000 and 20,000 ships in FoV as a function of the number of antennas, respectively. *SU* denotes the single user receiver with one antenna. *MU* denotes the receiver with directly applied ACMA and no interference suppression. *MU+SI* denotes the receiver with our beamforming algorithm proposed in [15]. *GSVD-T* denotes the receivers with our proposed GSVD tracking algorithm. GSVD-T gives the best performance at the lowest complexity. MU fails when the number of antennas grows because it gives its rank estimate $\hat{d}_s$ larger than that from MU+SI and GSVD-T. ACMA requires $\hat{d}_s^2 + 1$ samples to compute the beamformers but the lengths of the messages are limited.

Second, we build an experimental receiver for testing the proposed algorithms on real-world AIS signals. We use 4 antennas to collect the digitized baseband samples of the signals. The antennas are roughly spaced at half wavelengths. The RF equipment for the 4 antennas is not identical and calibrated. The receiver is put at altitude 68 meters high on the 17th floor of our building facing southwest, directly to the harbor of Rotterdam and the coastline about 10 nautical miles away. The receiver is behind two layers of window glasses and the metal frame of the building.

Fig. 4 shows the amplitude of the raw samples from the 4 antennas and one message separated from the other two partially overlapping messages in one analysis window. The oversampling ratio is 10 so the number of samples in one analysis window is 5120. The beamformers are computed from downsampled samples (downsampled by 10). The beamforming algorithm (or receiver) is GSVD-T but applied on one block data. It is seen in the upper figure that the antennas have different responses to the same message, which is mainly caused by the heavy fast fading in an urban environment. In the analysis window, one interference message overlaps the head

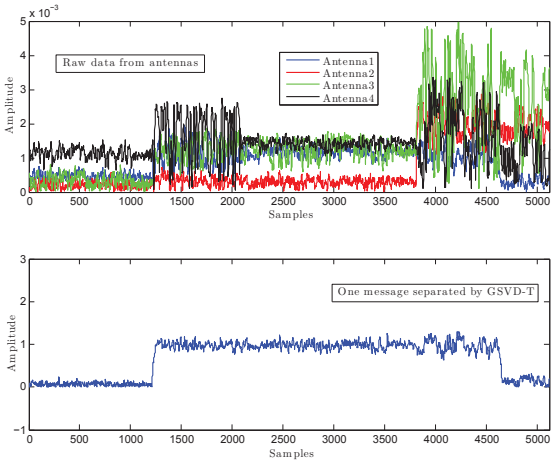

Fig. 4. An example of the proposed beamforming algorithm on real-world AIS signals.

of the middle message while another message overlaps the tail. The middle message is the target message in this analysis window. The lower figure shows the amplitude of the separated middle message. The input signal-to-interference ratio is below 0 dB and the output signal-to-interference-plus-noise ratio is above 10 dB. Without the beamforming algorithm, it is difficult to visually identify the start and the end of the middle message.

6 Conclusion

In this paper, we proposed simple and efficient beamforming techniques for AIS to suppress the interference caused by partially overlapping messages. The design principle of the proposed beamforming algorithms is based on the GSVD of two data blocks of the analysis window. The computation of the beamformer is through SURV for the subspace estimates from the GSVD is special cases of SSE-2. The proposed algorithms are directly applied to a tracking window. The simulation results and the test examples show that the proposed beamforming algorithms are effective to the two popular applications in AIS, on a satellite and in a ground base station.

7 REFERENCES

[1] O. F. H. Dahl, "Space-based AIS receiver for maritime traffic monitoring using interference cancellation," Master's thesis, Norwegian University of Science and Technology, Department of Electronics and Telecommunications, 2006.

[2] *REPORT ITU-R M.2084: Satellite detection of automatic identification system messages*, ITU Std., 2006.

[3] M. A. Cervera, A. Ginesi, and K. Eckstein, "Satellite-based vessel automatic identification system: A feasibility and performance analysis," *Int. J. Satell. Commun. Network.*, 2009.

[4] T. Eriksen, G. Høye, B. Narheim, and B. J. Meland, "Maritime traffic monitoring using a space-based AIS receiver," *Acta Astronautica*, vol. 58, no. 10, pp. 537–549, 2006.

[5] *RECOMMENDATION ITU-R M.1371-4: Technical characteristics for an automatic identification system using time-division multiple access in the VHF maritime mobile band*, ITU Std., 2010.

[6] M. Gallardo and U. Sorger, "Coherent receiver for AIS satellite detection," in *4th Int. Symp. on Commun., Control and Signal Process.*, Mar. 2010, pp. 1–4.

[7] D. J. Nelson and J. R. Hopkins, "GMSK co-channel demodulation," in *Proc. SPIE 7444*, 2009, p. 74440V.

[8] J. E. Hicks, J. S. Clark, J. Stocker, G. S. Mitchell, and P. Wyckoff, "AIS/GMSK receiver on FPGA platform for satellite application," in *Proc. SPIE 5819*, 2005, p. 403.

[9] P. Burzigotti, A. Ginesi, and G. Colavolpe, "Advanced receiver design for satellite-based automatic identification system signal detection," *International Journal of Satellite Communications and Networking*, vol. 30, no. 2, pp. 52–63, 2012.

[10] A. M. Kuzminskiy and Y. I. Abramovich, "Second-order asynchronous interference cancellation: Regularized semi-blind technique and non-asymptotic maximum likelihood benchmark," *Signal Processing*, vol. 86, no. 12, pp. 3849–3863, 2006.

[11] ——, "Non-stationary multiple-antenna interference cancellation for unsynchronized OFDM systems with distributed training," *Signal Processing*, vol. 89, no. 5, pp. 753–764, 2009.

[12] Y. Lee, R. Chandrasekaran, and J. Shynk, "Separation of cochannel GSM signals using an adaptive array," *IEEE Trans. Signal Process.*, vol. 47, no. 7, pp. 1977–1987, Jul. 1999.

[13] C. Budianu and L. Tong, "Channel estimation under asynchronous packet interference," *IEEE Trans. Signal Process.*, vol. 53, no. 1, pp. 333–345, Jan. 2005.

[14] M. Picard, M. Oularbi, G. Flandin, and S. Houcke, "An adaptive multi-user multi-antenna receiver for satellite-based AIS detection," in *Advanced Satellite Multimedia Systems Conference (ASMS) and 12th Signal Processing for Space Communications Workshop (SPSC), 2012 6th*, 2012, pp. 273–280.

[15] M. Zhou, A.-J. van der Veen, and R. van Leuken, "Multi-user LEO-satellite receiver for robust space detection of AIS messages," in *Proc. IEEE Int. Conf. Acoust., Speech, Signal Process.*, Kyoto, Japan, Mar. 2012.

[16] M. Simon and C. Wang, "Differential detection of Gaussian MSK in a mobile radio environment," *IEEE Trans. Veh. Technol.*, vol. 33, no. 4, pp. 307–320, Nov. 1984.

[17] R. Behrens and L. Scharf, "Signal processing applications of oblique projection operators," *IEEE Trans. Signal Process.*, vol. 42, no. 6, pp. 1413–1424, Jun. 1994.

[18] P. Hansen and S. Jensen, "Prewhitening for rank-deficient noise in subspace methods for noise reduction," *IEEE Trans. Signal Process.*, vol. 53, no. 10, pp. 3718–3726, 2005.

[19] A.-J. van der Veen, "A Schur method for low-rank matrix approximation," *SIAM J. Matrix Anal. Appl.*, vol. 17, no. 1, pp. 139–160, 1996.

[20] M. Zhou and A.-J. van der Veen, "Stable subspace tracking algorithm based on signed URV decomposition," in *Proc. IEEE Int. Conf. Acoust., Speech, Signal Process.*, Prague, Czech Republic, May 2011, pp. 2720–2723.

[21] A.-J. van der Veen and A. Paulraj, "An analytical constant modulus algorithm," *IEEE Trans. Signal Process.*, vol. 44, no. 5, pp. 1136–1155, May 1996.

[22] M. Zhou and A.-J. van der Veen, "A subspace tracking algorithm for separating partially overlapping data packets," in *Proc. of the Seventh IEEE Sensor Array and Multichannel Signal Process. Workshop (SAM)*, Hoboken, NJ, USA, Jun. 2012.

[23] M. Zhou and R. van Leuken, "SystemC-AMS model of a dynamic large-scale satellite-based AIS-like network," in *Forum on specification and Design Languages*, Oldenburg, Germany, Sept. 2011, pp. 24–31.